MPMI Vol. 35, No. 7, 2022, pp. 604–615, https://doi.org/10.1094/MPMI-02-22-0051-FI

e-Xtra*

Salt- and Osmo-Responsive Sensor Histidine Kinases Activate the *Bradyrhizobium diazoefficiens* General Stress Response to Initiate Functional Symbiosis

Janine Wülser,[1] Chantal Ernst,[1] Dominik Vetsch,[1] Barbara Emmenegger,[1] Anja Michel,[1] Stefanie Lutz,[2] Christian H. Ahrens,[2] Julia A. Vorholt,[1] Raphael Ledermann,[1,†] and Hans-Martin Fischer[1,†]

[1] Institute of Microbiology, ETH Zurich, CH-8093 Zürich, Switzerland
[2] Agroscope, Research Group Molecular Diagnostics, Genomics and Bioinformatics and Swiss Institute of Bioinformatics, CH-8820 Wädenswil, Switzerland

Accepted 22 March 2022.

The general stress response (GSR) enables bacteria to sense and overcome a variety of environmental stresses. In alphaproteobacteria, stress-perceiving histidine kinases of the HWE and HisKA_2 families trigger a signaling cascade that leads to phosphorylation of the response regulator PhyR and, consequently, to activation of the GSR σ factor σ^{EcfG}. In the nitrogen-fixing bacterium *Bradyrhizobium diazoefficiens*, PhyR and σ^{EcfG} are crucial for tolerance against a variety of stresses under free-living conditions and also for efficient infection of its symbiotic host soybean. However, the molecular players involved in stress perception and activation of the GSR remained largely unknown. In this work, we first showed that a mutant variant of PhyR where the conserved phosphorylatable aspartate residue D194 was replaced by alanine ($PhyR^{D194A}$) failed to complement the Δ*phyR* mutant in symbiosis, confirming that PhyR acts as a response regulator. To identify the PhyR-activating kinases in the nitrogen-fixing symbiont, we constructed in-frame deletion mutants lacking single, distinct combinations, or all of the 11 predicted HWE and HisKA_2 kinases, which we named HRXXN histidine kinases HhkA through HhkK. Phenotypic analysis of the mutants and complemented derivatives identified two functionally redundant kinases, HhkA and HhkE, that are required for nodulation competitiveness and during initiation of symbiosis. Using σ^{EcfG}-activity reporter strains, we further showed that both HhkA and HhkE activate the GSR in free-living cells exposed to salt and hyperosmotic stress. In conclusion, our data suggest that HhkA and HhkE trigger GSR activation in response to osmotically stressful conditions which *B. diazoefficiens* encounters during soybean host infection.

[†]Corresponding authors: R. Ledermann; raphael.ledermann@plants.ox.ac.uk, and H.-M. Fischer; fischeha@ethz.ch

Current address of R. Ledermann: Department of Plant Sciences, University of Oxford, Oxford, OX1 3RB, United Kingdom.

Funding: This work was supported by Schweizerischer Nationalfonds zur Förderung der Wissenschaftlichen Forschung (Swiss National Science Foundation) grants 31003A_153446/1 and 31003A_173255/1 and Eidgenössische Technische Hochschule Zürich.

*The *e*-Xtra logo stands for "electronic extra" and indicates that supplementary materials are published online.

The author(s) declare no conflict of interest.

Keywords: alphaproteobacteria, *Bradyrhizobium diazoefficiens*, general stress response, histidine kinase, multiple paralog knock-out, nitrogen fixation, nodulation, PhyR, σ^{EcfG}, soybean

To cope with challenging environmental conditions, bacteria have evolved a series of sophisticated stress response systems (Storz and Hengge 2011; Ron 2013). One prominent example is the so-called general stress response (GSR), which enables bacteria to integrate signals from a multitude of stress conditions and to mount a protective response not only against the inducing stress but also against other stresses unrelated to the inducing challenge (Fiebig et al. 2015; Francez-Charlot et al. 2015; Hengge 2011). In alphaproteobacteria, the GSR is controlled by a conserved regulatory system centered on the extracytoplasmic function (ECF) σ factor σ^{EcfG}, its anti-σ factor NepR, and the anti-σ factor antagonist PhyR (Fiebig et al. 2015; Francez-Charlot et al. 2015). The system is activated by stress-induced phosphorylation of PhyR at a conserved aspartate residue in its C-terminal receiver (REC) domain (Campagne et al. 2012; Francez-Charlot et al. 2009; Herrou et al. 2012). In the same studies, it was also shown that phosphorylation of PhyR triggers a conformational change leading to the exposure of its N-terminal σ factor-like output domain. Because NepR has higher binding affinity for the σ factor-like domain of PhyR than for σ^{EcfG}, a partner switch occurs, resulting in the release of σ^{EcfG}. Liberated σ^{EcfG} can bind to RNA polymerase core enzyme, mediating the recognition and activation of σ^{EcfG}-dependent promoters that are often associated with stress-related genes. Over the past decade, the signal transduction components acting upstream of the GSR master regulator PhyR and controlling its phosphorylation state have been elucidated in several alphaproteobacteria (Fiebig et al. 2015; Francez-Charlot et al. 2015; Staroń and Mascher 2010). Computational studies have identified sensor histidine kinases belonging to the HisKA_2 or HWE families as candidate components for the integration of GSR-activating stress signals, some of which have been experimentally validated thus far (Correa et al. 2013; Fiebig et al. 2019; Kaczmarczyk et al. 2014; Kim et al. 2014; Lori et al. 2018; Sauviac and Bruand 2014; Sycz et al. 2015; Tu et al. 2016). HisKA_2 and HWE kinases differ from classical HisKA kinases by a unique EXXHRXXN motif in the H-box of the dimerization and histidine phosphotransfer domain instead of the canonical H(E/D)LXXP motif (Grebe and Stock 1999; Herrou et al. 2017; Karniol and Vierstra 2004). Accordingly, and following the nomenclature of Kaczmarczyk et al. (2014), we refer to HisKA_2 and HWE kinases collectively as HRXXN kinases. In addition to

the characteristic H-box, HRXXN kinases share a glutamate instead of an asparagine in the N-box of the catalytic ATPase (HATPase_c) domain (EXXXN instead of NXXXN). HWE kinases are further characterized by two specific features displayed in their catalytic domain: an invariant histidine in the N-box (HEXXXN) and a WXE motif in the G1-box instead of the VXD motif present in HisKA_2 or classical HisKA kinases (Grebe and Stock 1999; Herrou et al. 2017; Karniol and Vierstra 2004).

HRXXN kinases are predominantly present in alphaproteobacteria, and many species encode numerous paralogs that may act in a functionally redundant manner (Herrou et al. 2017; Kaczmarczyk et al. 2014; Lori et al. 2018; Staroń and Mascher 2010). Some of the HRXXN kinases carry N-terminal sensory domains (Herrou et al. 2017), whereas others harbor an REC domain which is phosphorylated by an additional stress-perceiving kinase (Kaczmarczyk et al. 2015).

Although it was originally assumed that PhyR is phosphorylated directly by HRXXN kinases, recent findings indicated that phosphorylation of PhyR by HRXXN kinases in *Sphingomonas melonis* and *Caulobacter crescentus* can also occur indirectly, via a phosphorelay consisting of a single domain response regulator and a membrane-bound phosphotransferase harboring an HRXXN motif (Gottschlich et al. 2018; Lori et al. 2018). Notably, the respective HRXXN phosphotransferase PhyT of *S. melonis* has a degenerate catalytic domain (Kaczmarczyk et al. 2011).

Rhizobia consist of a subset of alpha- and betaproteobacteria with two fundamentally different lifestyles: they can occur either as free-living organisms in the soil or as nitrogen-fixing endosymbionts in root nodules of legume plants. The establishment of the mutually beneficial bacteria–plant interaction begins with the exchange of chemical signals; flavonoids secreted by the host plant are sensed by rhizobia which in return produce species-specific nodulation (Nod) factors (Oldroyd 2013; Walker et al. 2020; Wang et al. 2018). Nod factors induce the formation of root-nodule primordia. In addition, they trigger the curling of root hair cells, which consequently leads to entrapment of bacteria that form microcolonies. From these, bacteria invade the roots in plant-derived structures called infection threads which progress toward emerging nodule primordia where the bacteria infect and colonize root-nodule cells (Oldroyd et al. 2011; Tsyganova et al. 2021). Although nodule primordia develop into mature nodules, the rhizobia differentiate into bacteroids with the ability to convert atmospheric nitrogen into plant-available ammonia. In return, the host plant provides the bacteroids with reduced carbon and other nutrients (Ledermann et al. 2021b; Poole et al. 2018; Udvardi and Poole 2013). During both the free-living and symbiotic lifestyle, rhizobia experience a plethora of stresses. As soil inhabitants, they may be subject to desiccation, nutrient starvation, and shifts in temperature, osmolarity, and pH (Hirsch 2010; Shankar et al. 2021; Zahran 1999). During root invasion, they may encounter reactive oxygen species, nitric oxide, and plant defense responses (Benezech et al. 2020; Damiani et al. 2016; Gourion et al. 2015).

In our previous work, we addressed the role of the GSR in the soybean symbiont *Bradyrhizobium diazoefficiens*. GSR-deficient *B. diazoefficiens* mutants lacking PhyR or σ^{EcfG} show increased sensitivity against ionic and nonionic osmostress, alkaline pH, oxidative stress, desiccation, and heat shock under free-living conditions (Gourion et al. 2009; Ledermann et al. 2018, 2021a). Furthermore, these mutants are symbiotically defective, which is manifested by aberrant nodules and delayed nitrogen fixation. More specifically, we have shown that σ^{EcfG} is vital for infection thread formation and nodulation competitiveness. Consistent with these findings, GSR activity is increased in bacteria located in root-hair-entrapped microcolonies and infection threads. Most recently, we identified biosynthesis of the osmoprotectant trehalose as the GSR-controlled key function during early stages of host infection (Ledermann et al. 2021a). However, molecular components that sense and transduce stress signals to activate the PhyR-NepR-σ^{EcfG} cascade remained unknown. In the present study, we first demonstrate the critical role of *B. diazoefficiens* PhyR phosphorylation for stress protection and symbiosis. Furthermore, we describe the systematic mutational analysis of a set of 11 HRXXN kinases, which led to the identification of two members that are required for initiation of functional symbiosis as well as for salt- and osmostress-dependent GSR activation.

RESULTS

Phosphorylatable PhyR is required for GSR regulation in *B. diazoefficiens*.

First, we verified that PhyR requires phosphorylation to act as a response regulator in vivo. Amino acid sequence alignment of *B. diazoefficiens* PhyR with orthologs of other alphaproteobacteria revealed aspartate residue D194 located in the REC domain of *B. diazoefficiens* PhyR as the conserved phosphorylatable residue (Gourion et al. 2009; Herrou et al. 2010). Accordingly, a mutant allele of *phyR* (*phyR*^{D194A}) was constructed in which the aspartate residue D194 was changed to alanine. We tested whether either wild-type *phyR* (*phyR*^{wt}) or *phyR*^{D194A} can complement a Δ*phyR* mutant under hyperosmotic stress conditions and during symbiosis with soybean. Although *phyR*^{wt} restored wild type–like tolerance to hyperosmotic stress (400 mM sorbitol), *phyR*^{D194A} did not (Fig. 1A). The symbiotic properties of the complemented strains were determined in a soybean infection assay. The strain with reintroduced *phyR*^{wt} phenocopied the wild type with respect to nodule number, dry weight per nodule, nitrogenase activity per nodule dry weight, and nodule morphology (Fig. 1B to E). By contrast, the strain with *phyR*^{D194A} retained the Δ*phyR* mutant phenotype characterized by small, aberrant nodules lacking the red color originating from leghemoglobin and reduced nitrogen fixation. These results demonstrate that D194 is required for PhyR activity in vivo and they support the model of a phosphorylation-dependent activation mechanism of PhyR in *B. diazoefficiens*.

B. diazoefficiens encodes 12 HRXXN proteins.

By analogy with other alphaproteobacteria, HRXXN kinases are assumed to activate the GSR in *B. diazoefficiens*. A motif search for the characteristic EXXHRXXN motif identified 12 HRXXN proteins in the genome of *B. diazoefficiens* (Supplementary Table S1; Supplementary Fig. S1), 11 of which were termed HRXXN histidine kinase (Hhk)A to HhkK. Except for HhkK, all Hhk proteins harbor a conserved N-box motif in their catalytic domain (EXXXN) (Supplementary Fig. S1A). In HhkK, the catalytic domain is truncated and lacks the conserved N-box asparagine residue, making the presumed kinase activity of HhkK unlikely. The 12th identified HRXXN protein, Blr1461, also harbors a degenerate N-box, with the conserved asparagine replaced by a histidine (EXXXH). Blr1461 has a protein topology similar to that of the phosphotransferase PhyT of *S. melonis* (Gottschlich et al. 2018) and its gene can only be deleted in a GSR-deficient background (data not shown), consistent with the idea that it acts as an essential negative regulator of the GSR. Thus, Blr1461 was not classified as an Hhk protein.

Eight of the HRXXN proteins (HhkA, HhkC, HhkD, HhkH, HhkI, HhkJ, HhkK, and Blr1461) belong to the HWE family and four of them to the HisKA_2 family (HhkB, HhkE, HhkF, and HhkG). Although HhkA, HhkD, and Blr1461 are part of predicted transmembrane domains, the other HRXXN proteins are likely soluble and localized in the cytoplasm (Supplementary Table S1; Supplementary Fig. S1B). Some of the HRXXN proteins harbor sensory domains (GAF, PAS-PAC, and CHASE) or a phosphoryl group-accepting REC domain. Notably, *hhkE* is located in a putative operon with genes encoding a classical

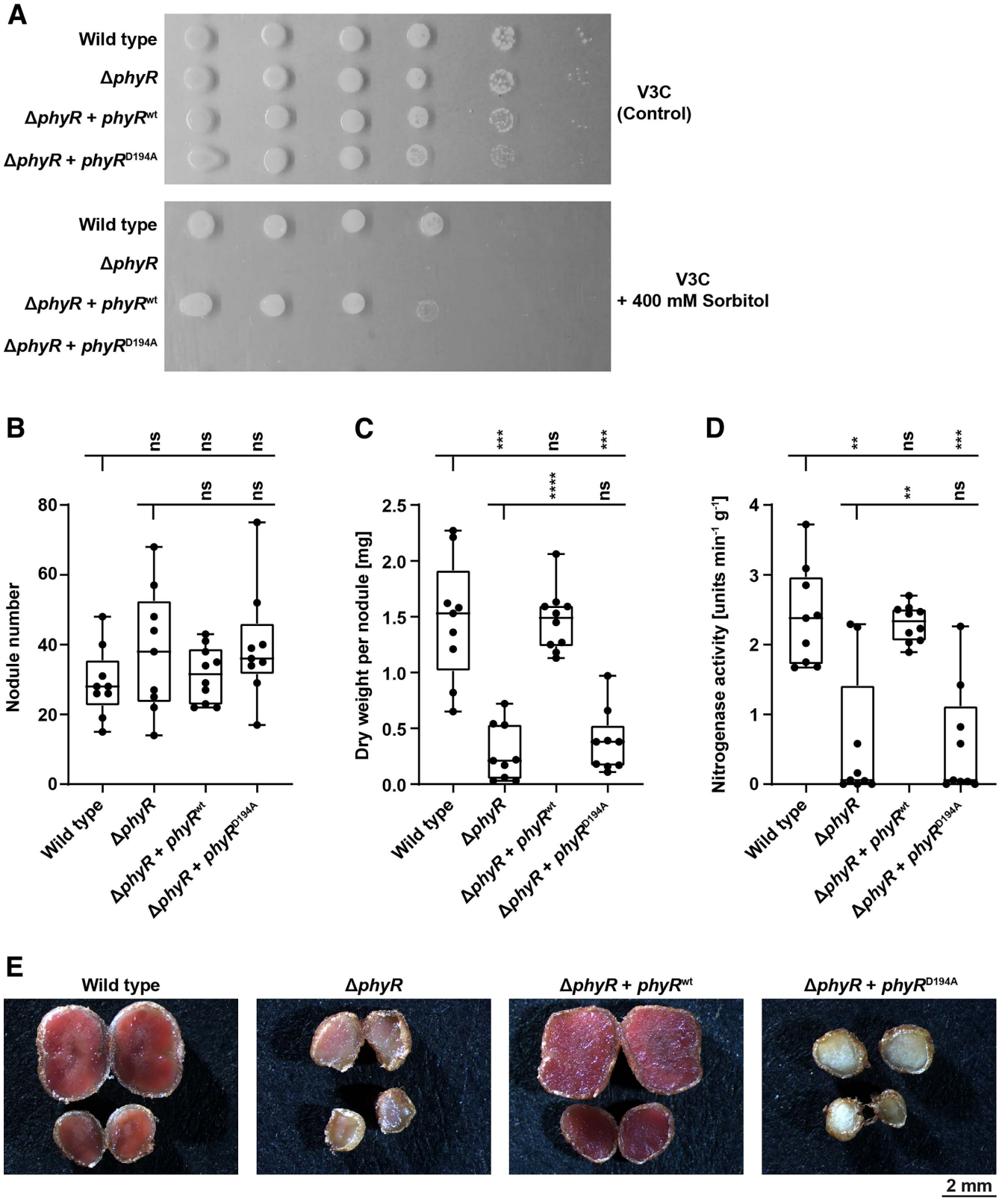

Fig. 1. Conserved aspartate residue D194 of PhyR is required for tolerance to hyperosmotic stress and functional symbiosis. **A,** Aliquots (4 µl each) of 10-fold serial dilutions (optical density at 600 nm $OD_{600} = 10^{-1}$ to 10^{-6}) of *Bradyrhizobium diazoefficiens* wild type (strain 110*spc*4), Δ*phyR* mutant (8402), Δ*phyR* mutant harboring either wild-type *phyR* (02-28; designated Δ*phyR* + *phyR*^{wt}), or *phyR*^{D194A} coding for a mutant variant of PhyR with the conserved aspartate residue D194 replaced by alanine (02-29; Δ*phyR* + *phyR*^{D194A}) were spotted on V3C agar plates containing no stressor (control) or 400 mM sorbitol (hyperosmotic stress). **B to E,** Following inoculation protocol 1 (see Materials and Methods), soybean seedlings (Green Butterbean) were inoculated with the same *B. diazoefficiens* strains used in A. Plants were harvested and evaluated 21 days postinoculation. **B,** Number and, **C,** dry weight of detachable nodules, including emerging and aborted nodules. **D,** Nitrogenase activity measured by acetylene reduction. **E,** Cross sections of nodules induced by the indicated strains. Values shown (B to D) originate from at least nine individual plants inoculated with the indicated strains. Box plots depict the median and the first and third quartiles, with whiskers extending to the most extreme data points. Strains marked with a vertical tick were statistically compared with strains under horizontal lines using one-way analysis of variance (ANOVA) (Brown-Forsythe and Welch ANOVA tests with Dunnett's T3 multiple comparison correction); ns = not significant ($P > 0.05$) and asterisks *, **, ***, and **** indicate $P \leq 0.05$, 0.01, 0.001, and 0.0001, respectively.

HisKA kinase (bll4289) and a single domain response regulator (bll4288) (Supplementary Fig. S1C). In analogy to the functionally studied homologs in *S. melonis* (Kaczmarczyk et al. 2015), we hypothesize that these two proteins are involved in HhkE-mediated signal integration (see Discussion).

Systematic mutagenesis of *hhk* genes to unravel their role in symbiosis.

First, markerless in-frame deletion mutants were constructed for each *hhk* gene. Because we obtained evidence for functional redundancy in initial phenotypic characterization experiments (unpublished data; see below), markerless multiple *hhk* deletion mutants were generated (Table 1). Having in mind that the sequential construction of 11 in-frame deletions includes the risk for accumulation of random off-target mutations, the *hhk* mutants were generated in two parallel approaches, starting from either *hhkA* or *hhkK*. In addition to intermediate constructs lacking different combinations of *hhk* genes, the mutagenesis strategy ultimately yielded two independent, formally identical strains that we named Δ11 and ΔXI, respectively, both lacking all 11 *hhk* genes. Genomic sequencing of the Δ11 and ΔXI mutants and comparison with the parental wild-type strain 110*spc*4 (Fernández et al. 2019) confirmed the 11 in-frame *hhk* gene deletions in both strains and did not reveal any common off-target mutations with a potential significant impact (e.g., frame-shift mutations or premature stop codons). Next, we tested the symbiotic phenotype of the two undecuple mutants Δ11 and ΔXI on soybean. Both showed congruent results and a striking symbiotically defective phenotype, manifested by reduced nitrogenase activity 14 days postinoculation (dpi) that matched the Δ*phyR* and Δ*ecfG* phenotype (Supplementary Fig. S2) (for more detailed phenotypes, see below) (Gourion et al. 2009, Ledermann et al. 2018). These results highlight the importance of the *hhk* genes for formation of functional symbiosis.

HhkA and HhkE contribute to symbiotic competitiveness.

To test whether all Hhk proteins are required for efficient symbiosis or only a subset, a competition assay for nodule occupancy was performed using selected mutants lacking specific subsets or all *hhk* genes. With this approach, we assessed the overall symbiotic fitness during multiple stages of the infection process. Soybean seedlings were inoculated with a 1:1 mixture of the LacZ-tagged wild type and either the GusA-tagged wild type or Δ*phyR* or Δ*hhk* mutants (Supplementary Fig. S3). When competing with the wild type, the Δ*phyR* mutant was severely impaired (Fig. 2), which is in agreement with previously described symbiotic defects of GSR mutants (Gourion et al. 2009; Ledermann et al. 2018). Likewise, both mutants lacking the complete set of *hhk* genes (Δ11 and ΔXI) showed a strongly reduced competitiveness, similar to the Δ*phyR* mutant (Fig. 2A and C). The mutant lacking *hhkA*, *hhkB*, and *hhkD* (Δ*hhkABD*) was competitive but the mutant additionally lacking *hhkE* (Δ*hhkABDE*) was much less so (Fig. 2B). A similar drop in competitiveness was observed upon deletion of *hhkA* in the Δ*hhkKJIHGFEDB* mutant (Fig. 2C). Together, these findings provide evidence that HhkA and HhkE contribute to competitiveness in a functionally redundant manner during establishment of the symbiosis.

HhkA and HhkE are key players for formation of functional symbiosis under noncompetitive conditions.

To further investigate the role of HhkA and HhkE during the symbiotic interaction, we constructed a deletion mutant strain lacking only these two kinases (Δ*hhkAE*). In addition, the Δ11 mutant was complemented by reinsertion of *hhkA* (Δ11 + *hhkA*), *hhkE* (Δ11 + *hhkE*), or both (Δ11 + *hhkAE*) at their original loci, thereby enabling expression from their native promoter (Table 1). We then determined the symbiotic properties of selected *hhk* mutant strains in a single-strain inoculation assay. At 12 dpi, the Δ11 mutant showed a symbiotic defect compared with the wild type, manifested by a reduced dry weight per nodule and nitrogenase activity (Fig. 3). In addition, nodules induced by the Δ11 mutant displayed reduced reddish coloration (Fig. 3D), indicating diminished leghemoglobin content. We noted that the symbiotic defect of the Δ11 mutant was not as pronounced as the one of the Δ*ecfG* and Δ*phyR* mutants. This was further substantiated by the fact that the Δ11 mutant showed wild type–like properties 21 dpi, whereas the Δ*phyR* mutant was still impaired at this timepoint (Supplementary Fig. S4). In contrast to the Δ11 mutant, single Δ*hhkA* and Δ*hhkE* mutants reached wild type–like nitrogenase activities 12 dpi and the respective nodules had a reddish interior, indicating normal levels of leghemoglobin (Fig. 3C and D). However, the double mutant lacking both *hhkA* and *hhkE* displayed a symbiotic defect that was almost as pronounced as that of the Δ11 mutant. Finally, complementation of the Δ11 mutant with either *hhkA*, *hhkE*, or both (Δ11 + *hhkA*, Δ11 + *hhkE*, or Δ11 + *hhkAE*) restored normal nodule formation and nitrogen fixation. Thus, out of the 11 Hhk proteins of *B. diazoefficiens*, HhkA and HhkE are crucial and sufficient for formation of efficient symbiosis and functionally redundant.

HhkA and HhkE activate the GSR in response to salt and hyperosmotic stress.

Given their importance during symbiosis, we aimed to characterize HhkA and HhkE with regard to their involvement in GSR activation in response to free-living stresses. For this purpose, we used the previously described β-galactosidase-based reporter system to monitor σ^{EcfG} activity (Ledermann et al. 2018). The *lacZYA* reporter cassette was integrated into the genome of selected *hhk* mutant strains downstream of the σ^{EcfG}-dependent gene bll6649 (Table 1). Because HhkE is a homolog of the salt-responsive kinase PakF of *S. melonis* (Kaczmarczyk et al. 2014, 2015) (see Discussion), we tested the resulting set of σ^{EcfG} activity reporter strains for their responsiveness to salt stress by exposing cells to 40 mM NaCl for 2 h, which did not interfere with viability of the cells (Supplementary Fig. S5A). Salt stress activated the reporter fusion in the wild type 4.6-fold (Fig. 4A). In contrast, no or only very weak activation was observed in the Δ*ecfG* and Δ*phyR* mutants, and likewise in the Δ11 mutant. When the Δ*hhkA*, Δ*hhkE*, and Δ*hhkAE* mutants were exposed to the same stress regime, the GSR was activated in all three mutants but only weakly in the double mutant, indicating the importance of both HhkA and HhkE in salt stress–mediated GSR activation. These findings were further substantiated by the fact that complementation of the Δ11 mutant with either *hhkA*, *hhkE*, or both resulted in NaCl stress-triggered GSR induction, though to varying degrees (2.7-, 4.8-, and 5.7-fold induction for *hhkA*, *hhkE*, and *hhkAE*, respectively) (Fig. 4A). We additionally studied the role of HhkA and HhkE in the GSR responsiveness to nonionic hyperosmotic stress at a sublethal concentration (400 mM sorbitol, 12 h) (Supplementary Fig. S5B). By monitoring the reporter fusion activity in sorbitol-stressed single and double *hhk* mutants, we showed that the respective kinases HhkA and HhkE also mediate GSR activation in response to nonionic osmostress (Fig. 4B). Consistent with these findings, *hhkA* and *hhkE* alone or in combination complemented the Δ11 mutant; however, unlike in the salt stress experiment, only partial complementation was observed in all strains.

DISCUSSION

The GSR core regulators PhyR and σ^{EcfG} are important for protection from stresses under free-living conditions and establishment of the symbiotic interaction between *B. diazoefficiens* and its leguminous host plants (Gourion et al. 2009; Ledermann

Table 1. Bacterial strains

Strain	Relevant phenotype or genotype[a]	Source or reference
Escherichia coli		
DH5α	*supE44* Δ*lacU169* (φ80 *lacZ*ΔM15) *hsdR17 recA1 gyrA96 thi-1 relA2*	BRL, Gaithersburg, MD, U.S.A.
S17-1 λ*pir*	Sm^r Sp^r *hsdR* (RP4-2 *kan*::Tn*7 tet*::*Mu*; chromosomally integrated)	de Lorenzo et al. 1993
Bradyrhizobium diazoefficiens		
110*spc*4	Sp^r wild type (USDA 110 derivative)	Regensburger and Hennecke 1983
8402	Sp^r Km^r Δ*phyR*::*aphII*	Gourion et al. 2009
8404	Sp^r Km^r Δ*ecfG*::*aphII*	Gourion et al. 2009
LacZYA-1	Sp^r Tc^r 110*spc*4 with P_{aphII}-*lacZYA* integrated ds of *scoI*	Ledermann et al. 2015
9937	Sp^r Tc^r 110*spc*4 with chromosomal integration of pRJ9937 (bll6649-*lacZYA*)	Ledermann et al. 2018
04-37	Sp^r Km^r Tc^r 8404 with chromosomal integration of pRJ9937 (bll6649-*lacZYA*)	Ledermann et al. 2018
02-28	Sp^r Km^r Tc^r 8402 with chromosomal integration of pRJ4728 ds of *scoI* (= Δ*phyR* + $phyR^{wt}$)[b]	This work
02-29	Sp^r Km^r Tc^r 8402 with chromosomal integration of pRJ4729 ds of *scoI* (= Δ*phyR* + $phyR^{D194A}$)[b]	This work
9910	Sp^r Δ*hhkA*	This work
9921	Sp^r Δ*hhkE*	This work
10-21	Sp^r Δ*hhkA* Δ*hhkE* (= Δ*hhkAE*)[b,c,d]	This work
hhkABD	Sp^r Δ*hhkA* Δ*hhkB* Δ*hhkD* (= Δ*hhkABD*)[b,c,d]	This work
hhkA-E	Sp^r Δ*hhkA* Δ*hhkB* Δ*hhkD* Δ*hhkE* (= Δ*hhkABDE*)[b,c,d]	This work
hhkK-B	Sp^r Δ*hhkK* Δ*hhkJ* Δ*hhkI* Δ*hhkH* Δ*hhkG* Δ*hhkF* Δ*hhkE* Δ*hhkD* Δ*hhkB* (= Δ*hhkKJIHGFEDB*)[b,c,d]	This work
hhkK-A	Sp^r Δ*hhkK* Δ*hhkJ* Δ*hhkI* Δ*hhkH* Δ*hhkG* Δ*hhkF* Δ*hhkE* Δ*hhkD* Δ*hhkB* Δ*hhkA* (= Δ*hhkKJIHGFEDBA*)[b,c,d]	This work
Δ11	Sp^r Δ*hhkA* Δ*hhkB* Δ*hhkD* Δ*hhkE* Δ*hhkF* Δ*hhkG* Δ*hhkH* Δ*hhkI* Δ*hhkJ* Δ*hhkK* Δ*hhkC*[c]	This work
ΔXI	Sp^r Δ*hhkK* Δ*hhkJ* Δ*hhkI* Δ*hhkH* Δ*hhkG* Δ*hhkF* Δ*hhkE* Δ*hhkD* Δ*hhkB* Δ*hhkA* Δ*hhkC*[c]	This work
Δ11-99	Sp^r Δ11 with chromosomal integration of *hhkA* (present on pRJ4799) at its original locus (= Δ11 + *hhkA*)[b]	This work
Δ11-01	Sp^r Δ11 with chromosomal integration of *hhkE* (present on pRJ4801) at its original locus (= Δ11 + *hhkE*)[b]	This work
Δ11-99-01	Sp^r Δ11-99 with chromosomal integration of *hhkE* (present on pRJ4801) at its original locus (= Δ11 + *hhkAE*)[b,d]	This work
mChegusA-1	Sp^r Tc^r 110*spc*4 with chromosomal integration of pRJPaph-mChe_a1-gusA ds of *scoI*	This work
02-mChegusA-1	Sp^r Km^r Tc^r 8402 with chromosomal integration of pRJPaph-mChe_a1-gusA ds of *scoI*	This work
Δ11-mChegusA-1	Sp^r Tc^r Δ11 with chromosomal integration of pRJPaph-mChe_a1-gusA ds of *scoI*	This work
hhkABD-mChegusA-1	Sp^r Tc^r hhkABD with chromosomal integration of pRJPaph-mChe_a1-gusA ds of *scoI*	This work
hhkAE-mChegusA-1	Sp^r Tc^r hhkA-E with chromosomal integration of pRJPaph-mChe_a1-gusA ds of *scoI*	This work
hhkKB-mChegusA-1	Sp^r Tc^r hhkK-B with chromosomal integration of pRJPaph-mChe_a1-gusA ds of *scoI*	This work
hhkKA-mChegusA-1	Sp^r Tc^r hhkK-A with chromosomal integration of pRJPaph-mChe_a1-gusA ds of *scoI*	This work
ΔXI-mChegusA-1	Sp^r Tc^r ΔXI with chromosomal integration of pRJPaph-mChe_a1-gusA ds of *scoI*	This work
02-37	Sp^r Km^r Tc^r 8402 with chromosomal integration of pRJ9937 (bll6649-*lacZYA*)	This work
10-37	Sp^r Tc^r 9910 with chromosomal integration of pRJ9937 (bll6649-*lacZYA*)	This work
21-37	Sp^r Tc^r 9921 with chromosomal integration of pRJ9937 (bll6649-*lacZYA*)	This work
10-21-37	Sp^r Tc^r 10-21 with chromosomal integration of pRJ9937 (bll6649-*lacZYA*)	This work
Δ11-37	Sp^r Tc^r Δ11 with chromosomal integration of pRJ9937 (bll6649-*lacZYA*)	This work
Δ11-99-37	Sp^r Tc^r Δ11-99 with chromosomal integration of pRJ9937 (bll6649-*lacZYA*)	This work
Δ11-01-37	Sp^r Tc^r Δ11-01 with chromosomal integration of pRJ9937 (bll6649-*lacZYA*)	This work
Δ11-99-01-37	Sp^r Tc^r Δ11-99-01 with chromosomal integration of pRJ9937 (bll6649-*lacZYA*)	This work

[a] Abbreviations: Sm^r, Sp^r, Km^r, and Tc^r = resistant to streptomycin, spectinomycin, kanamycin, and tetracycline, respectively; P = promoter and ds = downstream.
[b] To be concise, the abbreviated genotype indicated in parenthesis is used in the text, figures, and captions.
[c] Individual HRXXN histidine kinase (*hhk*) genes were deleted sequentially in the indicated order.
[d] Note that the abbreviated genotype indicated in parenthesis should not imply that the respective *hhk* genes are organized in operons.

et al. 2018). In the present study, we identified HRXXN kinases that control the activation of the PhyR-NepR-σ^{EcfG} cascade in response to stressful conditions.

First, we demonstrated that the conserved aspartate residue D194 of *B. diazoefficiens* PhyR is essential for tolerance to hyperosmotic stress as well as for functional symbiosis. This result is in line with previous in vitro protein–protein interaction studies demonstrating phosphorylation-dependent complex formation of *B. diazoefficiens* PhyR with NepR (Gourion et al. 2009). Together, these findings underline conservation of the phosphorylation-triggered activation mechanism of the PhyR-NepR-σ^{EcfG} cascade in *B. diazoefficiens* and suggest that PhyR phosphorylation involves stress-perceiving HRXXN kinases, as shown previously for *S. melonis* and *C. crescentus* (Kaczmarczyk et al. 2014; Lori et al. 2018). Accordingly, we aimed to unravel the role of 11 potentially GSR-activating HRXXN proteins (HhkA to HhkK) during the *B. diazoefficiens*–soybean symbiosis. A recently developed markerless-mutagenesis tool (Ledermann et al. 2016) enabled the systematic generation of a set of single and different combinatorial *hhk* mutants, including two strains (Δ11 and ΔXI) in which all 11 *hhk* genes were deleted following two independent, complementary mutagenesis routes. To our knowledge, this is the first time that such a large number of HRXXN protein-encoding genes in an alphaproteobacterium have been deleted and, likewise, 11 distinct genomic regions in a *Bradyrhizobium* sp. Notably, a comparable multiple deletion mutant strain was generated in a systematic study of all 11 *Sinorhizobium meliloti* ECF-type σ factors (Lang et al. 2018). The undecuple *B. diazoefficiens* mutants lacking all *hhk* genes were symbiotically impaired compared with the wild type, as shown by reduced symbiotic competitiveness and a delay in nodule formation and onset of nitrogen fixation. The symbiotic delay was slightly less pronounced than in the Δ*phyR* and Δ*ecfG* mutants (Supplementary Fig. S4) (Gourion et al. 2009, Ledermann et al. 2018). This trend might be explained by minimal residual σ^{EcfG} activity in *hhk* undecuple mutants, which is absent in mutants lacking the regulatory core proteins σ^{EcfG} or PhyR. In any case, we showed that the *hhk* genes are crucial for formation of symbiosis but cannot formally exclude the presence of alternative enzymatic pathways for GSR activation; for example, via unidentified phosphodonors not addressed in our study. Though not explicitly investigated, it seems unlikely that *hhk* mutants are impaired in root colonization because we had shown previously that this stage of the *B. diazoefficiens*–host interaction is not dependent on a functional GSR (Ledermann et al. 2018). However, the extent to which the GSR affects survival in the soil remains to be shown.

We further revealed a critical role of HhkA and HhkE during early stages of symbiosis. In addition to these two key players, other Hhk proteins contribute marginally to the establishment of symbiosis, as inferred from the slightly improved symbiotic properties of the Δ*hhkAE* mutant compared with the Δ11 mutant. Likewise, the symbiosis-relevant kinases HhkA and HhkE also play an important role in GSR activation in free-living cells exposed to salt and hyperosmotic stress conditions. Residual GSR activity found in the Δ*hhkAE* mutant mediated by Hhk proteins other than HhkA and HhkE may explain why expression of *hhkA* and *hhkE* in the Δ11 mutant did not restore wild type–like GSR activity under sorbitol stress conditions. Notably, whereas HhkA and HhkE display functional redundancy during early symbiosis, HhkE activates the GSR to a higher level than HhkA in response to free-living salt and hyperosmotic stress. Together, these findings are reminiscent of those described for the seven partially redundant GSR-activating kinases of *Sphingomonas melonis* (Kaczmarczyk et al. 2014).

The finding that, among the 11 Hhk proteins, HhkA and HhkE are most relevant for the symbiotic interaction raises a question

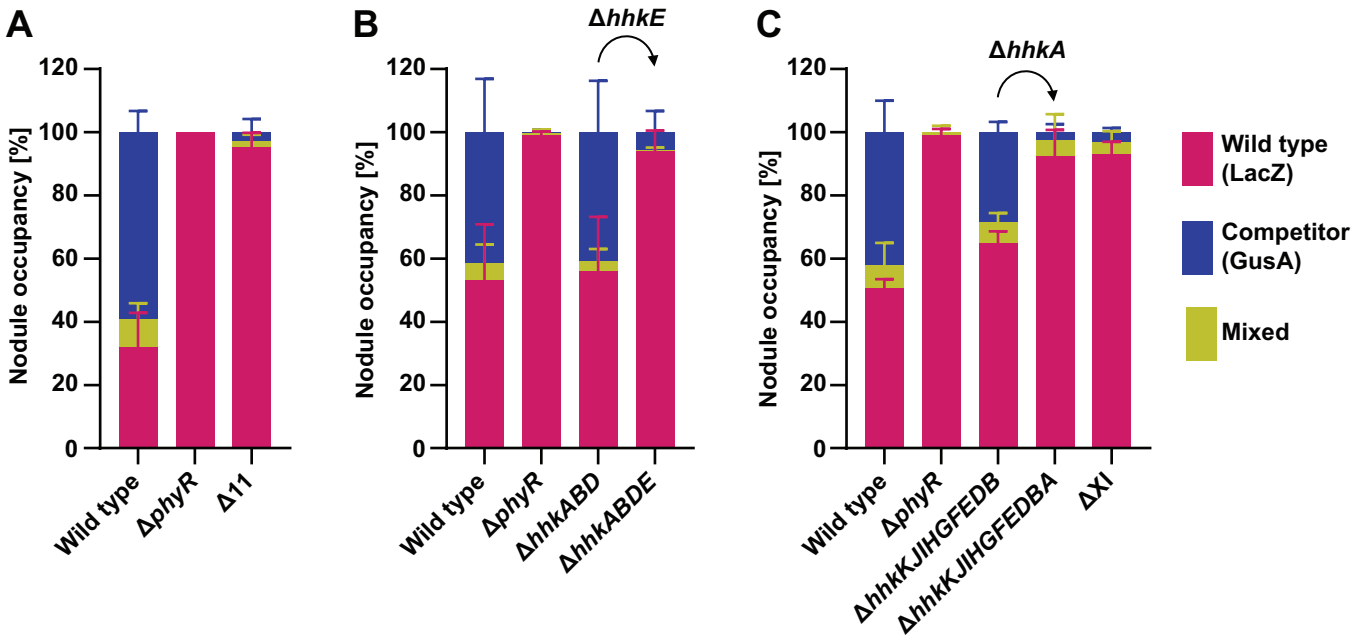

Fig. 2. HRXXN histidine kinase (Hhk)A and HhkE provide competitiveness during establishment of symbiosis. **A to C,** All strains indicated below the panels were tested against the LacZ-tagged wild type. To this end, two-day-old soybean seedlings of cultivars Green Butterbean (A and B) and Williams 82 (C) were planted into vermiculite and were inoculated with 1:1 mixtures (approximately 100 to 1,000 CFU in total) of the LacZ-tagged wild type (strain LacZYA-1) and the GusA-tagged wild type (mChegusA-1; control) or mutants Δ*phyR* (02-mChegusA-1), Δ11 (Δ11-mChegusA-1), Δ*hhkABD* (hhkABD-mChegusA-1), Δ*hhkABDE* (hhkAE-mChegusA-1), Δ*hhkKJIHGFEDB* (hhkKB-mChegusA-1), Δ*hhkKJIHGFEDBA* (hhkKA-mChegusA-1), or ΔXI (ΔXI-mChegusA-1). Plants were grown for 20 to 23 days before the nodules were harvested, cut in half, and stained for β-galactosidase and β-glucuronidase activity to identify nodule occupants. Whereas most of the nodules were colonized by only one strain, a few of them contained both competitors and, thus, were classified as "mixed". Data are based on the evaluation of the nodules of four plants per mixture, except for the combination wild type (LacZ) versus wild type (GusA) (C), where only three plants were analyzed. The mean and standard deviation of nodule occupancy of the indicated strains were plotted, and data for A, B, and C were generated in independent experiments.

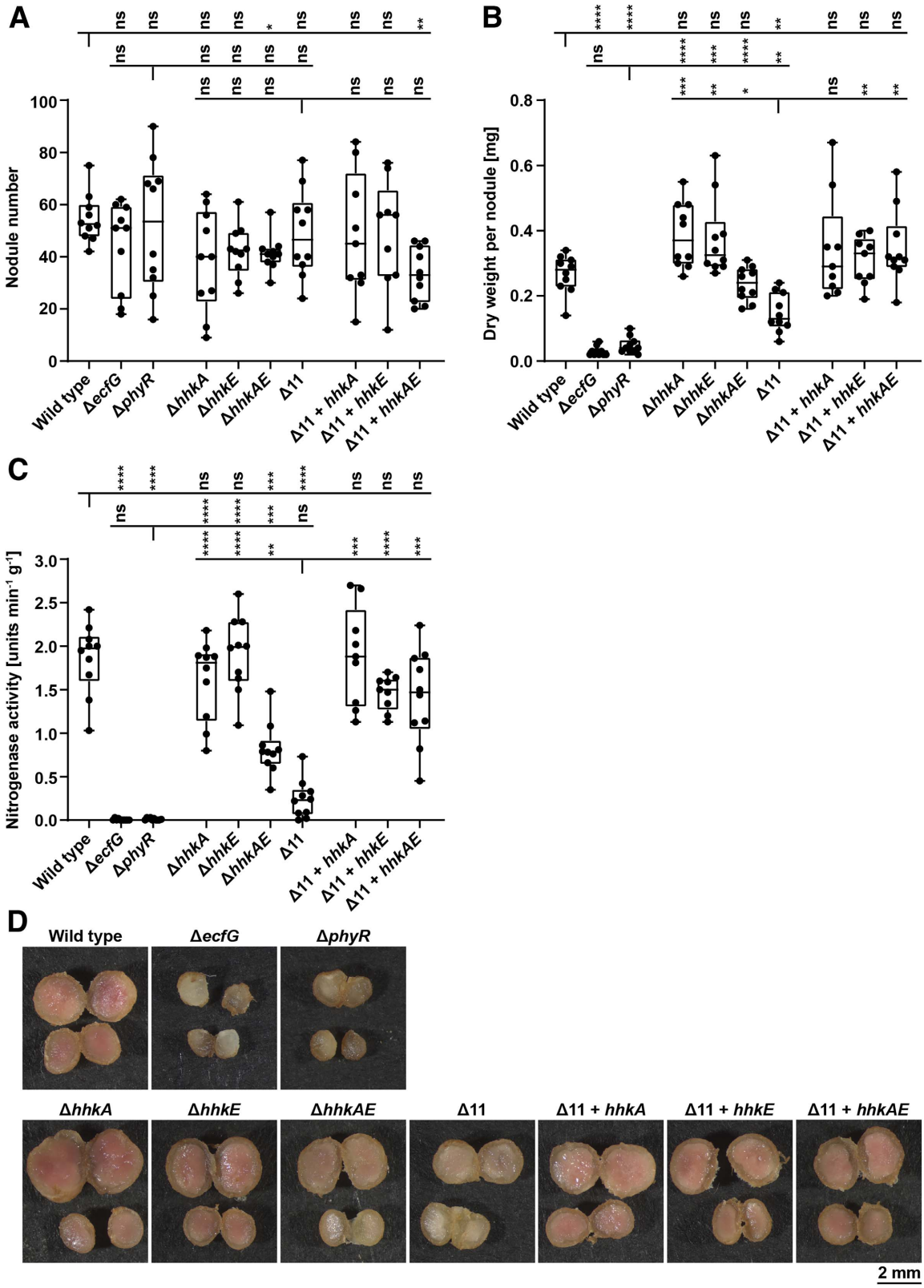

Fig. 3. HRXXN histidine kinase (Hhk)A and HhkE are crucial for formation of symbiosis. Following inoculation protocol 2 (see Materials and Methods), soybean seedlings (Williams 82) were inoculated with either of the following strains: *Bradyrhizobium diazoefficiens* wild type (strain 110*spc*4); mutants Δ*ecfG* (8404), Δ*phyR* (8402), Δ*hhkA* (9910), Δ*hhkE* (9921), Δ*hhkAE* (10-21), or Δ11; or the Δ11 mutant complemented with either *hhkA* (Δ11-99; designated Δ11 + *hhkA*), *hhkE* (Δ11-01; Δ11 + *hhkE*), or both (Δ11-99-01; Δ11 + *hhkAE*) inserted at their original loci. Plants were harvested and evaluated 12 days postinoculation. **A,** Number and, **B,** dry weight of detachable nodules, including emerging and aborted nodules. **C,** Nitrogenase activity measured by acetylene reduction. **D,** Cross sections of nodules induced by the indicated strains. Values shown (A to C) originate from at least nine individual plants inoculated with the indicated strains. Box plots depict the median, the first and third quartiles, and whiskers extending to the most extreme data points. Strains marked with a vertical tick were statistically compared with strains under horizontal lines using one-way analysis of variance (ANOVA) (Brown-Forsythe and Welch ANOVA tests with Dunnett's T3 multiple comparison correction); ns = not significant ($P > 0.05$) and asterisks *, **, ***, and **** indicate $P \leq 0.05$, 0.01, 0.001, and 0.0001, respectively.

about the unique properties of these two kinases. Higher expression of *hhkA* and *hhkE* compared with the remaining nine *hhk* genes is an unlikely explanation as deduced from previous transcriptomics data (Pessi et al. 2007). However, it is possible that the other Hhk proteins display either weaker enzymatic activity than HhkA and HhkE or none at all. Indeed, HRXXN kinases lacking the ability to autophosphorylate or transfer a phosphate group have been described for *C. crescentus* (Lori et al. 2018). This could also apply, for example, to HhkK, whose catalytic domain is degenerate (Supplementary Fig. S1A). Most critical for the significance of a particular kinase, however, is its ability to perceive the signal or signals generated by specific stress conditions. In analogy to *S. melonis*, different stress signals are expected to be perceived by different HRXXN kinases (Kaczmarczyk et al. 2014). Thus, whereas we propose that HhkA and HhkE integrate stress signals present at the onset of symbiosis, other Hhk proteins might respond to signals encountered by *B. diazoefficiens* in other stressful situations. It is likely that the stress

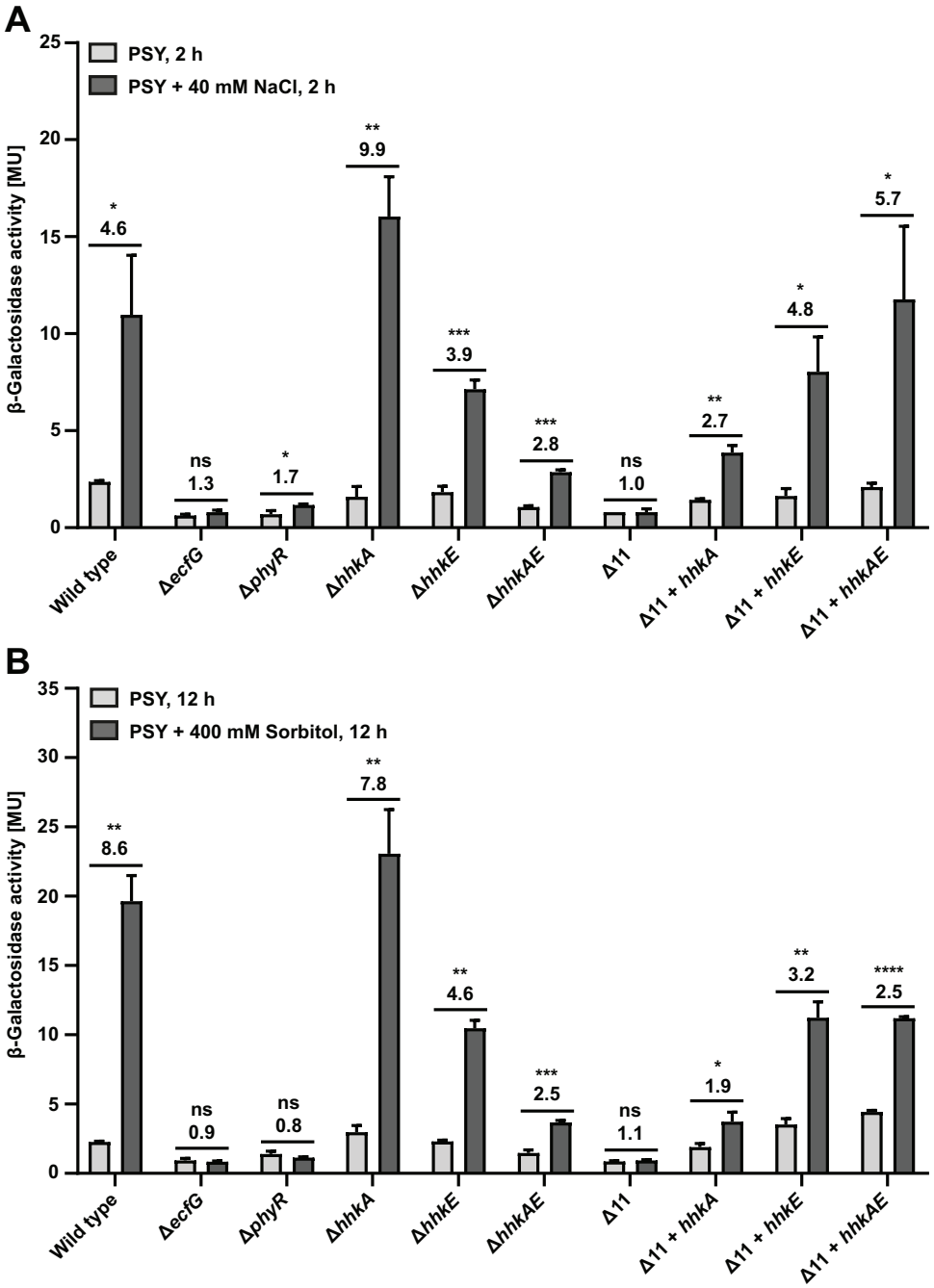

Fig. 4. HRXXN histidine kinase (Hhk)A and HhkE are involved in the response to salt and nonionic hyperosmotic stress. **A,** *Bradyrhizobium diazoefficiens* σ^{EcfG}-activity reporter strains containing a chromosomal σ^{EcfG}-dependent bll6649-*lacZYA* reporter fusion in a wild-type (strain 9937), Δ*ecfG* (04-37), Δ*phyR* (02-37), Δ*hhkA* (10-37), Δ*hhkE* (21-37), Δ*hhkAE* (10-21-37), Δ11 (Δ11-37), Δ11 + *hhkA* (Δ11-99-37), Δ11 + *hhkE* (Δ11-01-37), or Δ11 + *hhkAE* (Δ11-99-01-37) background were incubated under unstressed (peptone-salts-yeast extract [PSY] medium; $n = 3$) and salt stress (PSY + 40 mM NaCl; $n = 3$) conditions for 2 h or, **B,** under unstressed (PSY; $n = 3$) and hyperosmotic-stress (PSY + 400 mM sorbitol; $n = 3$) conditions for 12 h. Plotted are mean β-galactosidase activities of three biological replicates measured in two technical replicates, with error bars indicating the standard deviation. Adjacent columns under horizontal lines were statistically compared with a Welch's *t* test; ns = not significant ($P > 0.05$) and asterisks *, **, ***, and **** indicate $P \leq 0.05$, 0.01, 0.001, and 0.0001, respectively. Numbers above adjacent columns represent the calculated fold-change values between two compared conditions. Data in A and B originate from independent experiments.

signal specificity of a particular HRXXN kinase is reflected in its domain composition, yet neither HhkA nor HhkE harbor obvious sensory domains (Supplementary Table S1; Supplementary Fig. S1). Given the homology of HhkE and the genetically linked, classical HisKA kinase Bll4289 to their functionally studied *S. melonis* orthologs PakF and KipF, respectively (Kaczmarczyk et al. 2015), it is reasonable to assume that they operate in a two-tiered histidine kinase pathway. According to this model, the REC domain of HhkE is phosphorylated by Bll4289, which senses NaCl via its CHASE3 domain. In contrast to HhkE, no functionally analyzed homologs of HhkA are known and, thus, we can only speculate about its sensing and activation mechanism. Given the predicted HhkA topology (Supplementary Fig. S1B), salt or osmostress perception may involve the N-terminal transmembrane domains or the associated periplasmic loops (Schramke et al. 2016; Yuan et al. 2017). Conversely, it is formally possible that HhkA senses stresses via cytoplasmic regions (Kenney and Anand 2020) or via interaction with accessory proteins (Mascher 2014).

Apart from *B. diazoefficiens*, the GSR has been mainly studied in two other rhizobia; namely, *Sinorhizobium meliloti* and *Rhizobium etli.* In both species, GSR-controlling σ^{EcfG} homologs are required for tolerance of free-living cells to a variety of stressful conditions but, notably, not for functional symbiosis, even though genes in the GSR regulon are expressed during symbiosis. Likewise, an *Rhizobium leguminosarum* bv. *viciae* mutant lacking the EcfG-type σ factor RpoZ is symbiotically proficient (Meier et al. 2020; Sauviac et al. 2015).

Consistent with σ^{EcfG}-controlled GSR, HRXXN kinases are found in variable numbers in rhizobia (Supplementary Table S2). For example, *Sinorhizobium meliloti* encodes eight HRXXN proteins, of which at least two activate the GSR in response to free-living stress (Sauviac and Bruand 2014). Likewise, *R. leguminosarum* bv. *viciae* and *R. etli* harbor eight and seven genes, respectively, encoding HRXXN proteins. Given that GSR-deficient mutants of *Sinorhizobium meliloti* and *R. etli* form normal symbiosis with their respective hosts (Meier et al. 2020; Sauviac et al. 2015), their HRXXN kinases are likely dispensable for this lifestyle, though this remains to be confirmed. By contrast, the light-responsive HRXXN kinase R-LOV-HK of *R. leguminosarum* bv. *viciae* contributes to nodulation efficiency and competitiveness; however, its domain architecture is different from HhkA and HhkE and a link to GSR regulation is not known (Bonomi et al. 2012).

The prevalence of HhkA and HhkE-like proteins differs in the set of representative rhizobia listed in Supplementary Table S2. HhkA homologs are less widespread than HhkE homologs, which are often encoded downstream of two genes for a Bll4288-like single domain response regulator and a CHASE3 domain-containing HisKA kinase homologous to Bll4289. Because *R. etli* and *R. leguminosarum* bv. *viciae* lack obvious Bll4289 homologs, activation of their HhkE homologs might depend on other sensory kinases or phosphodonors.

Homologs of both HhkA and HhkE are also present in nonsymbiotic alphaproteobacteria and, again, HhkA homologs are less widespread than HhkE-like proteins. For example, HhkA homologs exist in the nonsymbiotic alphaproteobacteria *Afipia broomeae* and *Nitrobacter winogradskyi*, which are both phylogenetically closely related to *B. diazoefficiens*. Likewise, genetic modules resembling the bll4289-bll4288-*hhkE* locus in *B. diazoefficiens* are present in free-living alphaproteobacteria such as *S. melonis*, *Agrobacterium vitis*, or *Rhodobacter sphaeroides* (Kaczmarczyk et al. 2015).

Because HhkA and HhkE are found in rhizobia, which do not require a functional GSR for efficient symbiosis, as well as in nonsymbiotic bacteria, these kinases and the signals they integrate are unlikely to be symbiosis specific. In *B. diazoefficiens*, HhkA and HhkE are part of the GSR regulatory circuit, which is crucial for coping with stress conditions during early stages of host infection and also for free-living growth in unfavorable environments. Ledermann et al. (2021a) recently demonstrated that GSR-controlled biosynthesis of the osmostress protectant trehalose is crucial for efficient host infection by *B. diazoefficiens*. The responsiveness of HhkA and HhkE to ionic and hyperosmotic stress is consistent with the hypothesis that osmotic stress induces the GSR at the early stage of symbiosis. Thus, it will be interesting in the future to test whether bacteria pretreated by sublethal osmotic stress will exhibit elevated competitiveness and symbiotic performance. Although rhizobia are exposed to reactive oxygen species during early infection (Damiani et al. 2016; Gourion et al. 2015), it seems unlikely that this type of stress is sensed by one or several of the Hhk proteins because (i) the GSR is not activated by H_2O_2 (unpublished data), (ii) GSR-defective *B. diazoefficiens ecfG* and *phyR* mutants do not show elevated sensitivity to this stressor (Gourion et al. 2009), and (iii) *B. diazoefficiens* possesses other, GSR-independent systems to cope with oxidative stress (Masloboeva et al. 2012; Panek and O'Brian 2004). Further studies are required to find out by which other stresses the GSR in *B. diazoefficiens* can be induced and which Hhk proteins are responsible for the perception. Likewise, at this stage, it cannot be formally ruled out that Hhk proteins of *B. diazoefficiens* are involved in other signaling pathways in addition to the PhyR-NepR-σ^{EcfG} module at the GSR core.

MATERIALS AND METHODS

Bacterial strains and cultivation.

Bacterial strains used in this study are listed in Table 1. *Escherichia coli* was grown in Luria-Bertani medium (Miller 1972) at 37°C. When appropriate, antibiotics were added at the following concentrations: ampicillin (solid media, 200 μg ml^{-1} and liquid media, 100 μg ml^{-1}), streptomycin (50 μg ml^{-1}), and tetracycline (10 μg ml^{-1}). If not otherwise stated, *B. diazoefficiens* was routinely cultivated at 28 to 30°C in peptone-salts-yeast extract (PSY) medium containing 0.1% L-(+)-arabinose (Mesa et al. 2008) and, if appropriate, antibiotics were added at these concentrations: chloramphenicol (20 μg ml^{-1}; for counterselection of *E. coli* cells), kanamycin (100 μg ml^{-1}), spectinomycin (100 μg ml^{-1}), and tetracycline (solid media, 50 μg ml^{-1} and liquid media, 25 μg ml^{-1}).

Construction of plasmids and *B. diazoefficiens* mutant strains.

Cloning and mutagenesis procedures are summarized in this section; for further details, see Supplementary Materials. Primers used in this study and plasmids are listed in Supplementary Tables S3 and S4, respectively.

Mobilizable plasmids pRJ4728 and pRJ4729 encoding $phyR^{wt}$ and $phyR^{D194A}$, respectively, both under control of the native *phyR* promoter, were transferred via conjugation into the *B. diazoefficiens* Δ*phyR* mutant (strain 8402) and chromosomally integrated downstream of *scoI* as described previously (Ledermann et al. 2015). This resulted in strains 02-28 (designated Δ*phyR* + $phyR^{wt}$) and 02-29 (Δ*phyR* + $phyR^{D194A}$).

To generate markerless in-frame deletion mutants for the 12 HRXXN protein-encoding genes (*hhkA* through *hhkK* and blr1461) we used the pTETSIX system developed by Ledermann et al. (2016). Briefly, mutagenesis plasmids pRJ9910 through pRJ9921 were constructed, which consisted of a pTETSIX backbone carrying up- and downstream regions of individual *hhk* and blr1461 genes joined by a scar consisting of the first three and last three (including the stop) codons separated by a *Pac*I site plus one extra nucleotide to retain the reading frame. Upon mobilization of the mutagenesis plasmids to *B. diazoefficiens*, the targeted *hhk*

gene was deleted via two homologous recombination events, leaving behind the above-described scar. The genotype of candidate clones was confirmed by colony PCR. Genome sequencing, assembly, and annotation of mutant strains Δ11 and ΔXI lacking all 11 *hhk* genes were essentially performed as described previously (Fernández et al. 2019).

To integrate *hhkA* and *hhkE* at their original genomic location in the Δ11 mutant, we adapted the pTETSIX system. Plasmids pRJ4799 and pRJ4801, consisting of a pTETSIX backbone carrying *hhkA* or *hhkE*, respectively, including their up- and downstream regions, were constructed and mobilized into *B. diazoefficiens* strain Δ11. Selection of clones that had integrated *hhkA* or *hhkE* at their original genomic location via two homologous recombination events was performed as described (Ledermann et al. 2016), and the relevant genotype of candidate clones was verified by colony PCR.

B. diazoefficiens strains double tagged with mCherry and GusA, both under control of the constitutive P_{aphII} promoter, were generated by chromosomal integration of plasmid pRJPaph-mChe_a1-gusA in selected *B. diazoefficiens* strains downstream of *scoI*. The relevant genotype of resulting candidate clones was verified by colony PCR.

Construction of σ^{EcfG}-activity reporter strains followed a previously described protocol (Ledermann et al. 2018) and is further specified in the Supplementary Materials.

Plant infection tests.

Seeds of soybean (*Glycine max* (L.) Merr.) cultivar Green Butterbean (Johnny's Selected Seeds, Albion, ME, U.S.A.) were used for experiments shown in Figures 1 and 2A and B and Supplementary Fig. S2. At some point during our study, seeds of this soybean variety were no more commercially available. Thus, for experiments depicted in Figures 2C and 3 and Supplementary Fig. S4, we used seeds of soybean cultivar Williams 82 (kindly provided by D.-N. Rodriguez, CIFA, Las Torres-Tomejil, Seville, Spain), on which GSR-deficient *B. diazoefficiens* mutants were reported previously to have symbiotic defects (Gourion et al. 2009). Seeds were surface sterilized and germinated for 2 days according to our standard protocol (Ledermann et al. 2018). Plants were grown in plant growth chambers (Conviron) under the following conditions: 16-h light period at 28 to 29°C and 75% relative humidity, and 8-h dark period at 21 to 22°C and 90% relative humidity.

For the single-strain inoculation assays shown in Figure 1 and Supplementary Fig. S2, we applied our standard inoculation protocol (referred to as inoculation protocol 1). Specifically, 2-day-old seedlings were planted into vermiculite followed by inoculation with individual bacterial strains grown to exponential phase (1 ml of diluted bacterial suspension at an optical density at 600 nm [OD_{600}] = 0.01; approximately 10^7 CFU per seedling).

For optimal synchronization of plant growth and, thus, reducing variance between plants inoculated with the same strain, we used a slightly modified inoculation protocol (referred to as inoculation protocol 2) for the single-strain inoculation assays shown in Figure 3 and Supplementary Fig. S4. The 2-day-old seedlings were not directly inoculated but were grown axenically in vermiculite for 5 days before inoculation (for details, see protocol 1 above) with immediate watering with approximately 100 ml of sterile distilled water.

Depending on the specific experiment, plants were harvested 12, 14, or 21 dpi, and symbiotic properties were evaluated as reported (Fernández et al. 2019; Göttfert et al. 1990).

For competitive plant infection assays, bacterial cultures in the exponential growth phase were washed, diluted to 100 to 1,000 cells per milliliter, and CFU were determined by spotting aliquots on PSY agar plates. Using the suspensions with 100 to 1,000 cells per milliliter, 1:1 (vol/vol) mixtures of the LacZ-tagged wild type and either the GusA-tagged wild type, Δ*phyR* mutant, or selected Δ*hhk* mutants were prepared. Two-day-old soybean seedlings were planted into vermiculite and inoculated with 1 ml of the 1:1 mixtures. Nodules were harvested 20 to 23 dpi and stained for β-galactosidase and β-glucuronidase activity as previously described (Ledermann et al. 2015), with the following modifications: magenta-β-D-galactoside (Biosynth AG, Staad, Switzerland) was used instead of green-β-D-galactoside and nodules were stained overnight instead of for 4 h at 28°C. Stained nodules were preserved by placing them in 50% EtOH for 1 day and subsequent transfer to 70% EtOH before the number of magenta, blue, and two-colored ("mixed") nodules was determined.

Stress plate assays.

Bacterial cultures were grown in V3C medium, corresponding to Na_2-succinate-free V3S minimal medium (Canonica et al. 2019) supplemented with the following components: 0.5 g of yeast extract, 0.5 g of peptone, 1 mg of thiamin-HCl, 1 mg of biotin, 1 mg of D-pantothenic acid hemicalcium salt, and 3 g of L-(+)-arabinose per liter. Appropriate antibiotics were added at concentrations mentioned above. Exponential-phase cultures were harvested, washed, and adjusted to an OD_{600} of 0.1 and further serially diluted (1:10). Aliquots (4 µl each) of the dilution series were spotted on V3C agar plates lacking (control) or containing 400 mM sorbitol.

Monitoring σ^{EcfG} activity and viability of stressed and unstressed cells.

β-Galactosidase activity derived from σ^{EcfG}-dependent expression of a chromosomally integrated bll6649-*lacZYA* reporter fusion served as a proxy for σ^{EcfG} activity. Precultures of each reporter strain grown in PSY medium to the exponential growth phase were washed and used to inoculate fresh medium as follows. For salt stress experiments, six parallel cultures were inoculated in PSY medium to a starting OD_{600} of 0.2 and grown overnight. The next morning, NaCl (40 mM final concentration) was added to three of the cultures. Unstressed and NaCl-stressed cultures were incubated for two additional hours before β-galactosidase activity was determined. In a separate control experiment, CFU in unstressed and stressed cultures were determined at the start and at the end of the 2-h incubation period by spotting serial dilutions on PSY agar plates. For sorbitol stress experiments, the precultures were used to inoculate three parallel cultures in PSY medium and three parallel cultures in PSY medium supplemented with 400 mM sorbitol to a starting OD_{600} of 0.2. Cultures were incubated for 12 h before β-galactosidase activity was measured. In a separate control experiment, CFU were determined as described above at the beginning of and 14 h after sorbitol exposure. For β-galactosidase assays, cultures were harvested, washed, and resuspended in 0.9% NaCl solution. β-Galactosidase assays were performed as described previously (Miller 1972).

ACKNOWLEDGMENTS

We thank N. Holdener, J. E. Nathan, P. Peretti, S. Abele, and M. Bortfeld-Miller for experimental help; A. Schütz from the ETH Flow Cytometry Core Facility for support with FACS analysis; C. Vogel for advice on statistical data analysis; members of the Vorholt laboratory for help during harvest of plants; and L. Gottschlich, J.-M. Couzigou, G. Pessi, and X. Perret for fruitful discussions.

LITERATURE CITED

Benezech, C., Doudement, M., and Gourion, B. 2020. Legumes tolerance to rhizobia is not always observed and not always deserved. Cell. Microbiol. 22:e13124.

Bonomi, H. R., Posadas, D. M., Paris, G., Carrica, M. C., Frederickson, M., Pietrasanta, L. I., Bogomolni, R. A., Zorreguieta, A., and Goldbaum, F. A. 2012. Light regulates attachment, exopolysaccharide production, and nodulation in *Rhizobium leguminosarum* through a LOV-histidine kinase photoreceptor. Proc. Natl. Acad. Sci. U.S.A. 109:12135-12140.

Campagne, S., Damberger, F. F., Kaczmarczyk, A., Francez-Charlot, A., Allain, F. H. T., and Vorholt, J. A. 2012. Structural basis for sigma factor mimicry in the general stress response of Alphaproteobacteria. Proc. Natl. Acad. Sci. U.S.A. 109:E1405-E1414.

Canonica, F., Klose, D., Ledermann, R., Sauer, M. M., Abicht, H. K., Quade, N., Gossert, A. D., Chesnov, S., Fischer, H. M., Jeschke, G., Hennecke, H., and Glockshuber, R. 2019. Structural basis and mechanism for metallochaperone-assisted assembly of the Cu_A center in cytochrome oxidase. Sci. Adv. 5:eaaw8478.

Correa, F., Ko, W. H., Ocasio, V., Bogomolni, R. A., and Gardner, K. H. 2013. Blue light regulated two-component systems: Enzymatic and functional analyses of light-oxygen-voltage (LOV)-histidine kinases and downstream response regulators. Biochemistry 52:4656-4666.

Damiani, I., Pauly, N., Puppo, A., Brouquisse, R., and Boscari, A. 2016. Reactive oxygen species and nitric oxide control early steps of the legume - *Rhizobium* symbiotic interaction. Front. Plant Sci. 7:454.

de Lorenzo, V., Cases, I., Herrero, M., and Timmis, K. N. 1993. Early and late responses of TOL promoters to pathway inducers: Identification of postexponential promoters in *Pseudomonas putida* with *lacZ-tet* bicistronic reporters. J. Bacteriol. 175:6902-6907.

Fernández, N., Cabrera, J. J., Varadarajan, A. R., Lutz, S., Ledermann, R., Roschitzki, B., Eberl, L., Bedmar, E. J., Fischer, H. M., Pessi, G., Ahrens, C. H., and Mesa, S. 2019. An integrated systems approach unveils new aspects of microoxia-mediated regulation in *Bradyrhizobium diazoefficiens.* Front. Microbiol. 10:924.

Fiebig, A., Herrou, J., Willett, J., and Crosson, S. 2015. General stress signaling in the Alphaproteobacteria. Annu. Rev. Genet. 49:603-625.

Fiebig, A., Varesio, L. M., Alejandro Navarreto, X., and Crosson, S. 2019. Regulation of the *Erythrobacter litoralis* DSM 8509 general stress response by visible light. Mol. Microbiol. 112:442-460.

Francez-Charlot, A., Frunzke, J., Reichen, C., Ebneter, J. Z., Gourion, B., and Vorholt, J. A. 2009. Sigma factor mimicry involved in regulation of general stress response. Proc. Natl. Acad. Sci. U.S.A. 106:3467-3472.

Francez-Charlot, A., Kaczmarczyk, A., Fischer, H. M., and Vorholt, J. A. 2015. The general stress response in Alphaproteobacteria. Trends Microbiol. 23:164-171.

Göttfert, M., Hitz, S., and Hennecke, H. 1990. Identification of *nodS* and *nodU*, two inducible genes inserted between the *Bradyrhizobium japonicum nodYABC* and *nodIJ* genes. Mol. Plant-Microbe Interact. 3:308-316.

Gottschlich, L., Bortfeld-Miller, M., Gäbelein, C., Dintner, S., and Vorholt, J. A. 2018. Phosphorelay through the bifunctional phosphotransferase PhyT controls the general stress response in an alphaproteobacterium. PLoS Genet. 14:e1007294.

Gourion, B., Berrabah, F., Ratet, P., and Stacey, G. 2015. Rhizobium-legume symbioses: The crucial role of plant immunity. Trends Plant Sci. 20:186-194.

Gourion, B., Sulser, S., Frunzke, J., Francez-Charlot, A., Stiefel, P., Pessi, G., Vorholt, J. A., and Fischer, H. M. 2009. The PhyR-σ^{EcfG} signalling cascade is involved in stress response and symbiotic efficiency in *Bradyrhizobium japonicum.* Mol. Microbiol. 73:291-305.

Grebe, T. W., and Stock, J. B. 1999. The histidine protein kinase superfamily. Adv. Microb. Physiol. 41:139-227.

Hengge, R. 2011. The general stress response in gram-negative bacteria. Pages 251-289 in: Bacterial Stress Responses. G. Storz and R. Hengge, eds. ASM Press, Washington, DC, U.S.A.

Herrou, J., Crosson, S., and Fiebig, A. 2017. Structure and function of HWE/HisKA2-family sensor histidine kinases. Curr. Opin. Microbiol. 36:47-54.

Herrou, J., Foreman, R., Fiebig, A., and Crosson, S. 2010. A structural model of anti-anti-σ inhibition by a two-component receiver domain: The PhyR stress response regulator. Mol. Microbiol. 78:290-304.

Herrou, J., Rotskoff, G., Luo, Y., Roux, B., and Crosson, S. 2012. Structural basis of a protein partner switch that regulates the general stress response of α-proteobacteria. Proc. Natl. Acad. Sci. U.S.A. 109: E1415-E1423.

Hirsch, A. M. 2010. How rhizobia survive in the absence of a legume host, a stressful world indeed. Pages 375-391 in: Symbioses and Stress: Joint Ventures in Biology. J. Seckbach and M. Grube, eds. Springer, New York, NY, U.S.A.

Kaczmarczyk, A., Campagne, S., Danza, F., Metzger, L. C., Vorholt, J. A., and Francez-Charlot, A. 2011. Role of *Sphingomonas* sp. strain Fr1 PhyR-NepR-σ^{EcfG} cascade in general stress response and identification of a negative regulator of PhyR. J. Bacteriol. 193:6629-6638.

Kaczmarczyk, A., Hochstrasser, R., Vorholt, J. A., and Francez-Charlot, A. 2014. Complex two-component signaling regulates the general stress response in Alphaproteobacteria. Proc. Natl. Acad. Sci. U.S.A. 111:E5196-E5204.

Kaczmarczyk, A., Hochstrasser, R., Vorholt, J. A., and Francez-Charlot, A. 2015. Two-tiered histidine kinase pathway involved in heat shock and salt sensing in the general stress response of *Sphingomonas melonis* Fr1. J. Bacteriol. 197:1466-1477.

Karniol, B., and Vierstra, R. D. 2004. The HWE histidine kinases, a new family of bacterial two-component sensor kinases with potentially diverse roles in environmental signaling. J. Bacteriol. 186:445-453.

Kenney, L. J., and Anand, G. S. 2020. EnvZ/OmpR two-component signaling: An archetype system that can function noncanonically. EcoSal Plus 9:10.1128/ecosalplus.ESP-0001-2019.

Kim, H. S., Willett, J. W., Jain-Gupta, N., Fiebig, A., and Crosson, S. 2014. The *Brucella abortus* virulence regulator, LovhK, is a sensor kinase in the general stress response signalling pathway. Mol. Microbiol. 94:913-925.

Lang, C., Barnett, M. J., Fisher, R. F., Smith, L. S., Diodati, M. E., and Long, S. R. 2018. Most *Sinorhizobium meliloti* extracytoplasmic function sigma factors control accessory functions. MSphere 3:e00454-18.

Ledermann, R., Bartsch, I., Müller, B., Wülser, J., and Fischer, H. M. 2018. A functional general stress response of *Bradyrhizobium diazoefficiens* is required for early stages of host plant infection. Mol. Plant-Microbe Interact. 31:537-547.

Ledermann, R., Bartsch, I., Remus-Emsermann, M. N., Vorholt, J. A., and Fischer, H. M. 2015. Stable fluorescent and enzymatic tagging of *Bradyrhizobium diazoefficiens* to analyze host-plant infection and colonization. Mol. Plant-Microbe Interact. 28:959-967.

Ledermann, R., Emmenegger, B., Couzigou, J. M., Zamboni, N., Kiefer, P., Vorholt, J. A., and Fischer, H. M. 2021a. *Bradyrhizobium diazoefficiens* requires chemical chaperones to cope with osmotic stress during soybean infection. MBio 12:e00390-21.

Ledermann, R., Schulte, C. C. M., and Poole, P. S. 2021b. How rhizobia adapt to the nodule environment. J. Bacteriol. 203:e0053920.

Ledermann, R., Strebel, S., Kampik, C., and Fischer, H. M. 2016. Versatile vectors for efficient mutagenesis of *Bradyrhizobium diazoefficiens* and other alphaproteobacteria. Appl. Environ. Microbiol. 82:2791-2799.

Lori, C., Kaczmarczyk, A., de Jong, I., and Jenal, U. 2018. A single-domain response regulator functions as an integrating hub to coordinate general stress response and development in alphaproteobacteria. MBio 9:e00809-18.

Mascher, T. 2014. Bacterial (intramembrane-sensing) histidine kinases: Signal transfer rather than stimulus perception. Trends Microbiol. 22: 559-565.

Masloboeva, N., Reutimann, L., Stiefel, P., Follador, R., Leimer, N., Hennecke, H., Mesa, S., and Fischer, H. M. 2012. Reactive oxygen species-inducible ECF σ factors of *Bradyrhizobium japonicum.* PLoS One 7:e43421.

Meier, D., Casas-Pastor, D., Fritz, G., and Becker, A. 2020. Gene regulation by extracytoplasmic function (ECF) σ factors in alpha-rhizobia. Adv. Bot. Res. 94:289-321.

Mesa, S., Hauser, F., Friberg, M., Malaguti, E., Fischer, H. M., and Hennecke, H. 2008. Comprehensive assessment of the regulons controlled by the FixLJ-$FixK_2$-$FixK_1$ cascade in *Bradyrhizobium japonicum.* J. Bacteriol. 190:6568-6579.

Miller, J. H. 1972. Experiments in Molecular Genetics. Cold Spring Harbor Laboratory Press, Cold Spring Harbor, NY, U.S.A.

Oldroyd, G. E. D. 2013. Speak, friend, and enter: Signalling systems that promote beneficial symbiotic associations in plants. Nat. Rev. Microbiol. 11:252-263.

Oldroyd, G. E. D., Murray, J. D., Poole, P. S., and Downie, J. A. 2011. The rules of engagement in the legume-rhizobial symbiosis. Annu. Rev. Genet. 45:119-144.

Panek, H. R., and O'Brian, M. R. 2004. KatG is the primary detoxifier of hydrogen peroxide produced by aerobic metabolism in *Bradyrhizobium japonicum.* J. Bacteriol. 186:7874-7880.

Pessi, G., Ahrens, C. H., Rehrauer, H., Lindemann, A., Hauser, F., Fischer, H. M., and Hennecke, H. 2007. Genome-wide transcript analysis of *Bradyrhizobium japonicum* bacteroids in soybean root nodules. Mol. Plant-Microbe Interact. 20:1353-1363.

Poole, P., Ramachandran, V., and Terpolilli, J. 2018. Rhizobia: From saprophytes to endosymbionts. Nat. Rev. Microbiol. 16:291-303.

Regensburger, B., and Hennecke, H. 1983. RNA polymerase from *Rhizobium japonicum.* Arch. Microbiol. 135:103-109.

Ron, E. Z. 2013. Bacterial stress response. Pages 589-603 in: The Prokaryotes. E. Rosenberg, E. F. DeLong, S. Lory, E. Stackebrandt, and F. Thompson, eds. Springer, Berlin, Germany.

Sauviac, L., Bastiat, B., and Bruand, C. 2015. The general stress response in alpha-rhizobia. Pages 405-414 in: Biological Nitrogen Fixation. F. J. de Bruijn, ed. John Wiley & Sons, Inc., Hoboken, NJ, USA.

Sauviac, L., and Bruand, C. 2014. A putative bifunctional histidine kinase/phosphatase of the HWE family exerts positive and negative control on the *Sinorhizobium meliloti* general stress response. J. Bacteriol. 196:2526-2535.

Schramke, H., Tostevin, F., Heermann, R., Gerland, U., and Jung, K. 2016. A dual-sensing receptor confers robust cellular homeostasis. Cell Rep. 16:213-221.

Shankar, S., Haque, E., Ahmed, T., Kiran, G. S., Hassan, S., and Selvin, J. 2021. Rhizobia–legume symbiosis during environmental stress. Pages 201-220 in: Symbiotic Soil Microorganisms. N. Shrivastava, S. Mahajan, and A. Varma, eds. Soil Biology, vol. 60. Springer, Cham, Switzerland.

Staroń, A., and Mascher, T. 2010. General stress response in α-proteobacteria: PhyR and beyond. Mol. Microbiol. 78:271-277.

Storz, G., and Hengge, R., eds. 2011. Bacterial Stress Responses. ASM Press, Washington, DC, U.S.A.

Sycz, G., Carrica, M. C., Tseng, T. S., Bogomolni, R. A., Briggs, W. R., Goldbaum, F. A., and Paris, G. 2015. LOV histidine kinase modulates the general stress response system and affects the *virB* operon expression in *Brucella abortus.* PLoS One 10:e0124058.

Tsyganova, A. V., Brewin, N. J., and Tsyganov, V. E. 2021. Structure and development of the legume-rhizobial symbiotic interface in infection threads. Cells 10:1050.

Tu, N., Lima, A., Bandeali, Z., and Anderson, B. 2016. Characterization of the general stress response in *Bartonella henselae*. Microb. Pathog. 92:1-10.

Udvardi, M., and Poole, P. S. 2013. Transport and metabolism in legume-rhizobia symbioses. Annu. Rev. Plant Biol. 64:781-805.

Walker, L., Lagunas, B., and Gifford, M. L. 2020. Determinants of host range specificity in legume-rhizobia symbiosis. Front. Microbiol. 11: 585749.

Wang, Q., Liu, J., and Zhu, H. 2018. Genetic and molecular mechanisms underlying symbiotic specificity in legume-rhizobium interactions. Front. Plant Sci. 9:313.

Yuan, J., Jin, F., Glatter, T., and Sourjik, V. 2017. Osmosensing by the bacterial PhoQ/PhoP two-component system. Proc. Natl. Acad. Sci. U.S.A. 114:E10792-E10798.

Zahran, H. H. 1999. Rhizobium-legume symbiosis and nitrogen fixation under severe conditions and in an arid climate. Microbiol. Mol. Biol. Rev. 63:968-989.